Direct Yaw Moment Control for Electric Vehicles with Variable-Rate-Slip-Ratio-Limiter Based Driving Force Control

Takumi Ueno, Binh-Minh Nguyen, Hiroshi Fujimoto
The University of Tokyo
5-1-5, Kashiwanoha, Kashiwa, Chiba, 277-8561, Japan
ueno.takumi22@ae.k.u-tokyo.ac.jp, nguyen.binhminh@edu.k.u-tokyo.ac.jp, fujimoto@k.u-tokyo.ac.jp

***Abstract*—Yaw-rate control by direct yaw moment control (DYC) for in-wheel motor electric vehicles has been studied for years. However, how to properly treat the difference between the wheels' friction limit circles is still an open issue. For instance, in conventional methods, the yaw-rate might not follow the reference value due to the utilization of a fixed-slip-ratio-limiter regardless of the cornering operation. To deal with this problem, this paper proposes a new DYC method, which is based on driving force control with variable-rate-slip-ratio-limiter. To evaluate the effectiveness of the proposed method, simulation and experiment were conducted using a four-wheel vehicle under a low-friction surface condition. Experimental results show that, in comparison with the conventional method, the proposed method can reduce the root mean square deviation of the yaw-rate tracking error by $62.7\,\%$.**

***Index Terms*—Direct yaw moment control, Driving force control, Electric vehicles, Slip ratio control, Variable-rate-slip-ratio-limiter, Yaw-rate control**

I. Introduction

In order to achieve a decarbonized society by 2050, the automotive industry is shifting from conventional internal combustion engine vehicles to electric vehicles (EVs). EVs are not only environmentally friendly in terms of transportation, but also novel motion control systems, thanks to their fast and accurate torque generation capacity [1].

This study considers in-wheel motored EVs, which allow the torque to be independently controlled at each wheel. Thanks to this merit, direct yaw moment control (DYC) has been proposed to control the yaw-rate and improve the lateral stability of the vehicle. The DYC system is commonly designed with a yaw-rate controller in the outer-layer and a driving force controller (DFC) in the inner-layer.

From a literature review, many advanced methods have been proposed for the outer-layer [2]–[9]. Among them, yaw moment observer (YMO) can improve the robustness of the control system based on the concept of disturbance observer [10]. Besides, torque vectoring control is a combination of the DYC with an optimal torque distribution law to minimize the energy consumption of the vehicle [7]–[9]. Unfortunately, [2]–[9] are merely provided with a simple feedforward DFC in the inner-layer. For instance, the motor torque T is merely calculated as $T = rF$, where r is the wheel radius and F is the driving force. This simple control approach limits the accuracy of the actual yaw moment generated by motors.

To improve the traction control, many types of controllers have been proposed, such as fuzzy logic control [11], sliding mode control [12], and model predictive control [13]. Our research group originally developed the DFC [14], [15], which can accurately track the actual driving forces with the reference values. The DFC with a slip ratio limiter can also effectively prevent the EVs from slipping on the low-friction surface. However, the DFC has mainly been studied in the longitudinal motion of the EVs. Recently, Fuse *et al*. have utilized the varying slip ratio limiter on the DFC to improve the maneuverability of the EVs [16]. This approach allows the vehicle to extend the cornering force generation capability. How to implement DFC in the DYC framework is still an open issue. To this end, it is essential to address the variation of the friction limit circles, which could be very different between the left and right sides while cornering.

This paper is to develop a DYC based on the DFC. With respect to the aforementioned discussion, this paper focuses on the cornering motion of the vehicle on a low-friction surface. To deal with the difference between the left and right friction limit circles, a variable-rate-slip-ratio-limiter is introduced to the DFC configuration. The rate can be updated in real-time by utilizing the YMO and driving force observer (DFO). By using a four-wheel vehicle developed by our research group, the advantage of the proposed method has been proved in comparison with the conventional DYC.

The remainder of this paper is organized as follows. Section Ⅱ presents the dynamic model of the vehicle. The DYC system and the proposed variable-rate-slip-ratio-limiter are presented in Section Ⅲ. Simulation results are shown in Section Ⅳ, and the experimental results are demonstrated in Section V. Finally, the conclusion is drawn in Section Ⅵ.

II. Vehicle dynamics model

A. Lateral Motion of Vehicle Body

This paper investigates a planar vehicle model shown in Fig. 1. Based on this model, the equations of motion can be expressed as follows [17]:

$$MV\left(\frac{d\beta}{dt}+\gamma\right)=2(Y_f+Y_r+Y_d), \tag{1}$$

$$I\dot{\gamma}=N_z-N_t-N_d, \tag{2}$$

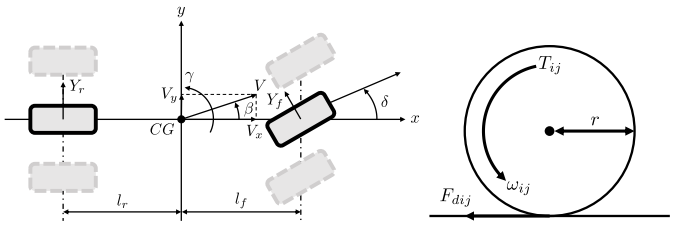

(a) Planar vehicle model. (b) Wheel rotational model.

Fig. 1. Vehicle model.

where M and I denote the vehicle mass and yaw moment of inertia, respectively. The vehicle speed, yaw-rate, and side slip angle are V, γ, and β, respectively. In addition, Y is the lateral force and the subscripts f and r denote the front and rear wheels, respectively. Y_d and N_d represent the lateral force and yaw moment disturbances, respectively. N_z is the yaw moment, which can be generated by the driving force difference between the left and right wheels. N_t is the moment generated by the lateral tire forces and is given by

$$N_t = 2l_r Y_r - 2l_f Y_f, \tag{3}$$

where l_f and l_r are the distances from the center of gravity (CG) to the front and rear wheel axles, respectively.

B. Rotational Motion of Wheels

The rotational motion of each wheel is described as

$$J_{ij}\dot{\omega}_{ij} = T_{ij} - r_{ij}F_{dij}, \tag{4}$$

where J is the wheel moment of inertia, r is the wheel radius, ω is the angular velocity, T is the motor torque, and F_d is the driving force (friction force). The subscription ij denotes the index of the wheel ($i = \{\text{front}, \text{rear}\}, j = \{\text{left}, \text{right}\}$). When the vehicle accelerates or decelerates, the wheel velocity $V_\omega = r\omega$ differs from the vehicle velocity V because of the tire's elastic deformation. The slip ratio λ is defined as

$$\lambda_{ij} = \frac{V_{\omega ij} - V}{\max(V_{\omega ij}, V, \epsilon)}, \tag{5}$$

where ϵ is a small positive value to prevent division by zero. The nonlinear relationship between the driving force and slip ratio is commonly described by Pacejka's magic formula [18]. When the slip ratio is small, this relationship can be linearized by $F_d = D_s\lambda$ where D_s is the driving stiffness which can be estimated from the experimental data.

III. PROPOSED DYC SYSTEM

Assuming a rear-wheel drive system, the block diagram of the proposed method is shown in Fig. 2, including two controller layers.

A. Outer–Layer : Yaw-rate Control

The yaw-rate reference can be calculated as

$$\gamma^* = \frac{1}{1 + AV^2}\frac{V}{l}\delta, \tag{6}$$

where δ is the steering angle of the front wheel, which is given by the driver, and $l = l_f + l_r$. The stability factor A is defined as

$$A = -\frac{M}{2l^2}\frac{l_f C_f - l_r C_r}{C_f C_r}, \tag{7}$$

where C denotes the cornering stiffness, which is obtained from experimental data by linearizing the lateral tire force model. The stability factor describes the steering characteristics of the vehicle. The vehicle can be classified into understeer or oversteer if the sign of A is $+$ or $-$, and the vehicle is neutral steer if A equals to 0. To improve the robustness of the yaw-rate control under the uncertainty of road conditions and the unknown disturbances Y_d, N_t, and N_d, the YMO is utilized. As shown in Fig. 2, the YMO is established with the nominal inertia I_n, and the ω_c is the cut-off frequency of the low-pass filter. N_{in} is the yaw moment generated by the feedforward controller and feedback controller. Let $\hat{N}_{dt}$ be the output of the YMO, we have $N_z^* = N_{in} + \hat{N}_{dt}$, which is the yaw moment command. Let F_{dall}^* and d be the total driving force command given by the driver and tread base, the force distribution law (FDL) is designed as

$$\begin{bmatrix} F_{dRL} \\ F_{dRR} \end{bmatrix} = \begin{bmatrix} 1/2 & 1/d \\ 1/2 & -1/d \end{bmatrix} \begin{bmatrix} F_{dall}^* \\ N_z^* \end{bmatrix}. \tag{8}$$

B. Inner–Layer : Driving Force Control

Each wheel is provided with the DFC. As shown in Fig. 2, the DFC has a cascade configuration, including an integral force controller and a proportional-integral wheel speed controller. The driving force is feedbacked thanks to the DFO, which utilizes the motor torque and the angular velocity of the wheel. Define the following variable as

$$y = \frac{V_\omega}{V} - 1. \tag{9}$$

With respect to (5) and (9), y is approximate the slip ratio in either acceleration or deceleration situations. Hence, it can be treated as an output of the DFC and can be used to calculate the reference angular velocity of the wheel.

C. Proposal of variable-rate-slip-ratio-limiter

In this subsection, we propose a method for varying the rate of slip ratio limiter in the DFC. In the previous studies in the DFC, the left and right side limiters are conventionally provided with a constant value. For instance, the limiters can be set as $\lambda_{limL} = \lambda_{limR} = 0.06$, a small value that guarantees the stable longitudinal motion of the vehicle on the low friction surface. However, the situation is quite different when the vehicle turns. The driving force F_d is limited by μF_z, where F_z is the vertical force and μ is the road friction coefficient. Due to the load transfer, the vertical forces of the left and right sides change with the situation. Therefore, the optimal driving force also changes in real-time. Consequently, the limited value of the slip ratio would be adaptively changing in real-time to optimize the yaw moment generation capability of the vehicle. As an example, Fig. 3 demonstrates the situation such that the vehicle turns left on the low friction roads. By setting

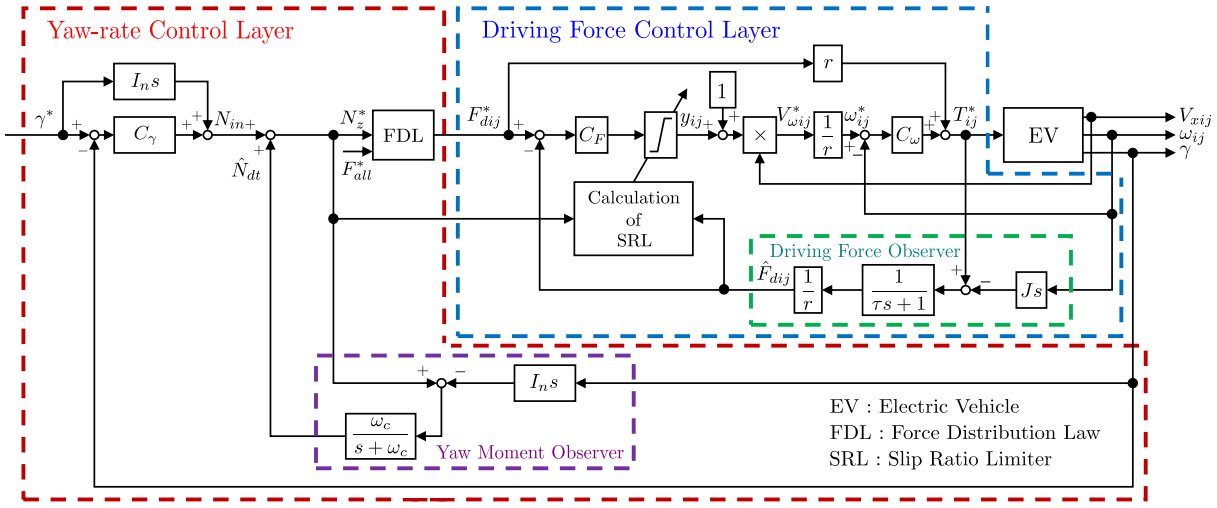

Fig. 2. Block diagram of the proposed DYC system.

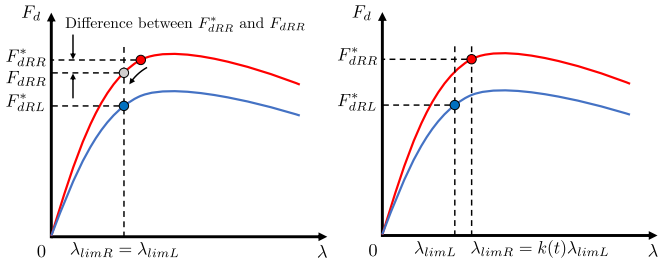

(a) Conventional method. (b) Proposed method.

Fig. 3. Example of the relationship between slip ratio and driving force (Left turn).

TABLE I
SIMULATED VEHICLE PARAMETER.

Symbol	Description	Value
M	Vehicle Mass	925 kg
r	Wheel Radius	0.302 m
J	Inertia of Wheel	1.2619 kgm^2
I	Inertia of Vehicle Body	617 kgm^2
d	Tread Base	1.3 m
l	Wheel Base	1.7 m
l_f	Distance between CG and Front Axle	0.988 m
l_r	Distance between CG and Rear Axle	0.712 m
C_f	Front Cornering Stiffness	2340 N/rad
C_r	Rear Cornering Stiffness	2940 N/rad

$\lambda_{limL} = \lambda_{limR}$, the existing DFC might not generate enough yaw moment, hence, degrading the cornering performance. In addition, it is so difficult to estimate μ-peak and dangerous to enter the nonlinear region of the tire that we have to set the limiter with a little extra margin. To deal with the aforementioned issue, we examine the mechanism to generate the ideal yaw moment, which is expressed by

$$N_z = -\frac{d}{2}(F_{dRL} - F_{dRR}). \tag{10}$$

We assume that the slip ratio is small. In the situation such that the wheel slips and reaches the limited value, the driving forces of the rear left and rear right wheels are expressed as

$$F_{dRL} = \lambda_{limL} D_{sL}, \tag{11}$$
$$F_{dRR} = \lambda_{limR} D_{sR}. \tag{12}$$

Let k be the rate between the left and right limiters, it can be given as

$$k(t) = \frac{\lambda_{limR}}{\lambda_{limL}}. \tag{13}$$

In this study, we assume that the road conditions are the same between the left and right wheels. Thus, we can approximately treat $D_{sL} = D_{sR}$. From (10)–(13), the rate $k(t)$ can be updated in real-time as

$$k(t) = \begin{cases} 1 + \frac{2N_z^*}{d\hat{F}_{dRL}} & (V \geq V_t) \\ 1 & (V < V_t) \end{cases}, \tag{14}$$

where N_z^* is given by the outer-layer, and $\hat{F}_{dRL}$ is given by the DFO. V_t is a threshold value to prevent the division by zero. By using this threshold value, we assume that if $V < V_t$, the driving force is small and close to zero. The proposed rate can be straightforwardly extended to the negative driving force situation (deceleration).

IV. SIMULATION

A. Simulation setup

The simulation model was established based on the four-wheel EV Kanon developed by our research group. In this study, this vehicle is utilized as a rear-drive system. The main parameters of the vehicle are listed in Tab. I. The simulation was performed as follows. The vehicle runs straight at the constant speed of 10 km/h on the road surface with the friction coefficient of 0.2. After 1 s, it turns left with a constant steering angle of 0.06 rad. Simultaneously, the vehicle accelerates with F_{dall}^* of 300 Nm. By a fine-tuning process, the proportional

TABLE II
RMSD OF YAW-RATE.

Method	RMSD of yaw-rate $\mathrm{rad/s}$	Rate of decrease $\%$
Case 1	7.97×10^{-4}	0
Case 2	6.07×10^{-4}	23.8
Case 3	1.07×10^{-4}	86.5

and integral gain of wheel angular velocity controller C_ω are selected as 50.476 and 504.76 respectively, and the integral gain of the DFC C_F is 0.003. In the outer-loop, the yaw-rate controller C_γ is selected as a proportional controller with the gain of 12340. Three test cases are conducted as follows.
- Case 1: The vehicle is handled by the driver (without yaw-rate control).
- Case 2: The vehicle is controlled by the DYC that utilizes the DFC with fixed-slip-ratio-limiter.
- Case 3: The vehicle is controlled by the proposed DYC.

B. Simulation result

Figures 4–6 demonstrate the simulation results of the three test cases, including the slip ratio and the rate of the limiters, the yaw moment, and the yaw-rate response. It can be seen that in Cases 1 and 2, the slip ratios of the rear left and rear right wheels are almost the same. In contrast, the slip ratio of the rear-right wheel is bigger than that of the rear-left wheel in Case 3. This is because we set $k(t)$ to generate the driving forces required by the yaw moment controller, and this value increases above 1 since 1 second. Thanks to this variant of $k(t)$, the difference between the actual and required yaw moments becomes smaller. Consequently, the proposed method can reduce the tracking error between the actual and reference yaw-rate.

V. EXPERIMENT

A. Experimental setup

Figure 7(a) shows the experimental EV FPEV2-Kanon, which was developed by our research group. This is a four-wheel drive in-wheel-motored electric vehicle. Each wheel is driven by a permanent-magnet synchronous motor. This vehicle is powered by a lithium-ion battery and equipped with a yaw-rate sensor. The test scenario and vehicle trajectory are demonstrated in Figs. 7(b) and 7(c), respectively. The polymer sheets covered by water were utilized to simulate the slippery road surface. The friction coefficient of this surface is about 0.2. In the simulation, a constant steering angle was given, whereas, in the experiment, the vehicle was handled to run on the predetermined turning path. The vehicle run straight at the speed of $10\,\mathrm{km/h}$ and makes a tip-in accelerated turn from $1\,\mathrm{s}$. For safety reasons, $k(t)$ is bounded between a lower bound of 0.5 and an upper bound of 10. In addition, the control gains are the same as these of the simulation.

B. Experimental result

The experimental results of the three cases are summarized in Figs. 8–10, respectively. The slip ratios are suppressed by about 0.06 in Case 1 (without yaw-rate control) and Case 2 (conventional DYC). By varying $k(t)$ in Case 3 (proposed DYC), the slip ratio is bigger than 0.06. It is assumed that the driving force of the outer wheel is increased, and the proposed method can reduce the difference between the actual and required yaw moments. The conventional DYC can follow the reference until around $2\,\mathrm{s}$, but it begins to deviate after that. On the other hand, the proposed control follow the reference value at all time. To evaluate the performance of the three methods, the root mean square deviation (RMSD) of the yaw-rate control errors is calculated from $1\,\mathrm{to}\,5\,\mathrm{s}$. The RMSD values are summarized in Tab. II. In comparison with Case 1 (without yaw-rate control), Case 2 (conventional DYC) can reduce the tracking error by $23.8\,\%$. Remarkably, the tracking error can be reduced by about $86.5\,\%$ by Case 3 (proposed DYC).

VI. CONCLUSION

In this paper, we proposed a new DYC system based on driving force control with the variable-rate-slip-ratio-limiter. The boundary of the limiter is updated in real-time by utilizing the yaw moment command and the estimated driving force. The effectiveness of the proposed method is evaluated by both simulation and experiment. The results show that the proposed method can operate effectively even when cornering with acceleration on the low friction surface. In the future, we will develop separate limiters for both the left and right wheels, and consider the split-μ scenario.

ACKNOWLEDGMENT

This work was partially supported by Tsugawa Foundation. In addition, it was partly supported by Industrial Technology Research Grant Program from New Energy and Industrial Technology Development Organization (NEDO) of Japan (number 05A48701d), the Ministry of Education, Culture, Sports, Science and Technology grant (number 22246057 and 26249061).

REFERENCES

[1] Y. Hori, "Future vehicle driven by electricity and control-research on four wheel motored, "UOT Electric March II"," in *7th International Workshop on Advanced Motion Control. Proceedings (Cat. No. 02TH8623)*. IEEE, 2002, pp. 1–14.

[2] B.-M. Nguyen, Y. Wang, H. Fujimoto, and Y. Hori, "Lateral stability control of electric vehicle based on disturbance accommodating kalman filter using the integration of single antenna gps receiver and yaw rate sensor," *Journal of electrical engineering and technology*, vol. 8, no. 4, pp. 899–910, 2013.

[3] S. Ding, L. Liu, and W. X. Zheng, "Sliding mode direct yaw-moment control design for in-wheel electric vehicles," *IEEE Transactions on Industrial Electronics*, vol. 64, no. 8, pp. 6752–6762, 2017.

[4] H. Zhang, J. Liang, H. Jiang, Y. Cai, and X. Xu, "Stability research of distributed drive electric vehicle by adaptive direct yaw moment control," *IEEE Access*, vol. 7, pp. 106 225–106 237, 2019.

[5] B. Lenzo, M. Zanchetta, A. Sorniotti, P. Gruber, and W. De Nijs, "Yaw rate and sideslip angle control through single input single output direct yaw moment control," *IEEE Transactions on Control Systems Technology*, vol. 29, no. 1, pp. 124–139, 2020.

[6] H. Fuse, H. Fujimoto, K. Sawase, N. Takahashi, R. Takahashi, Y. Okamura, and R. Koga, "Derivation of dynamic model of two-input-two-output torque difference amplification motor drive system and independent left-and-right wheel control with decoupling compensator," *IEEJ Journal of Industry Applications*, vol. 11, no. 3, pp. 427–436, 2022.

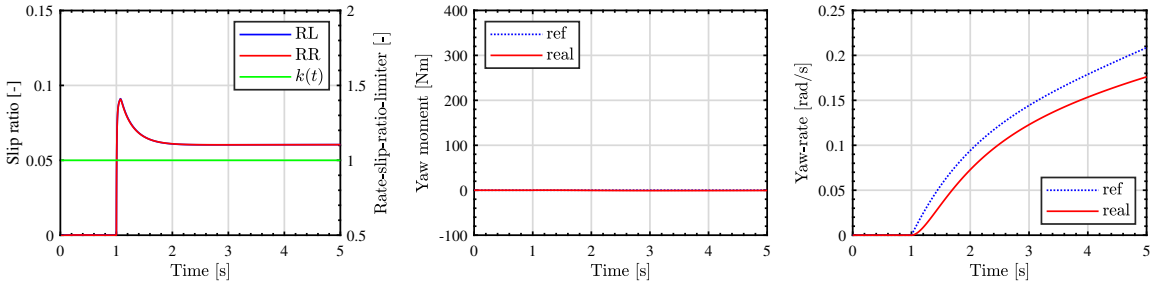

(a) Slip ratio and rate-slip-ratio-limiter. (b) Yaw moment. (c) Yaw-rate.

Fig. 4. Simulation result of Case 1 (without yaw-rate control).

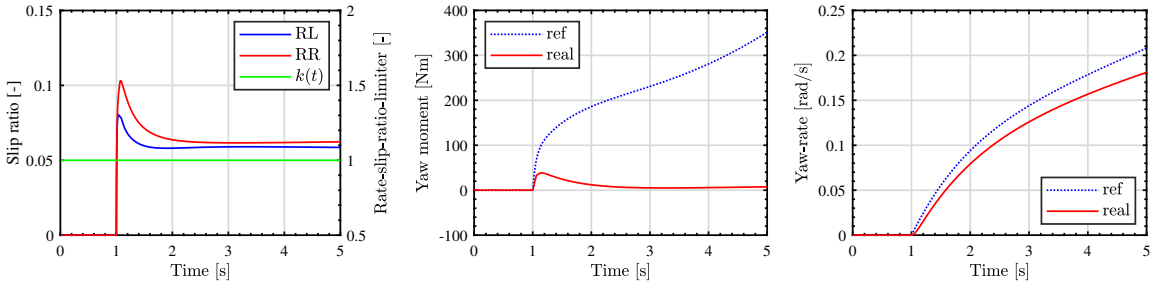

(a) Slip ratio and rate-slip-ratio-limiter. (b) Yaw moment. (c) Yaw-rate.

Fig. 5. Simulation result of Case 2 (conventional DYC).

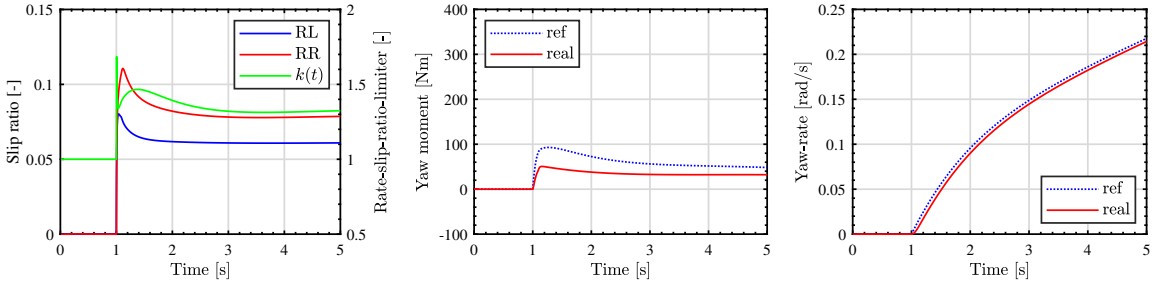

(a) Slip ratio and rate-slip-ratio-limiter. (b) Yaw moment. (c) Yaw-rate.

Fig. 6. Simulation result of Case 3 (proposed DYC).

[7] X. Hu, H. Chen, Z. Li, and P. Wang, "An energy-saving torque vectoring control strategy for electric vehicles considering handling stability under extreme conditions," *IEEE Transactions on Vehicular Technology*, vol. 69, no. 10, pp. 10 787–10 796, 2020.

[8] A. Mangia, B. Lenzo, and E. Sabbioni, "An integrated torque-vectoring control framework for electric vehicles featuring multiple handling and energy-efficiency modes selectable by the driver," *Meccanica*, vol. 56, no. 5, pp. 991–1010, 2021.

[9] M. Chae, Y. Hyun, K. Yi, and K. Nam, "Dynamic handling characteristics control of an in-wheel-motor driven electric vehicle based on multiple sliding mode control approach," *IEEE Access*, vol. 7, pp. 132 448–132 458, 2019.

[10] H. Fujimoto, T. Saito, and T. Noguchi, "Motion stabilization control of electric vehicle under snowy conditions based on yaw-moment observer," in *The 8th IEEE International Workshop on Advanced Motion Control, 2004. AMC'04.* IEEE, 2004, pp. 35–40.

[11] P. Khatun, C. M. Bingham, N. Schofield, and P. Mellor, "Application of fuzzy control algorithms for electric vehicle antilock braking/traction control systems," *IEEE Transactions on Vehicular Technology*, vol. 52, no. 5, pp. 1356–1364, 2003.

[12] D. Savitski, V. Ivanov, K. Augsburg, T. Emmei, H. Fuse, H. Fujimoto, and L. M. Fridman, "Wheel slip control for the electric vehicle with in-wheel motors: Variable structure and sliding mode methods," *IEEE Transactions on Industrial Electronics*, vol. 67, no. 10, pp. 8535–8544, 2019.

[13] Z. He, Q. Shi, Y. Wei, B. Gao, B. Zhu, and L. He, "A model predictive control approach with slip ratio estimation for electric motor antilock braking of battery electric vehicle," *IEEE Transactions on Industrial Electronics*, vol. 69, no. 9, pp. 9225–9234, 2021.

[14] M. Yoshimura and H. Fujimoto, "Driving torque control method for electric vehicle with in-wheel motors," *Electrical Engineering in Japan*, vol. 181, no. 3, pp. 49–58, 2012.

[15] H. Fujimoto, J. Amada, and K. Maeda, "Review of traction and braking control for electric vehicle," in *2012 IEEE Vehicle Power and Propulsion Conference*, 2012, pp. 1292–1299.

[16] H. Fuse and H. Fujimoto, "Cornering force maximization with variable slip ratio control for independent-all-wheel-drive electric vehicle," *IEEE Journal of Emerging and Selected Topics in Industrial Electronics*, 2022.

[17] M. Abe, "Vehicle motion and control, jidosha no undo to seigyo (in japanese)," 2008.

[18] H. Pacejka, *Tire and vehicle dynamics*. Elsevier, 2005.

(a) FPEV2-Kanon. (b) Test scenario. (c) Trajectory setting.

Fig. 7. Experimental setup.

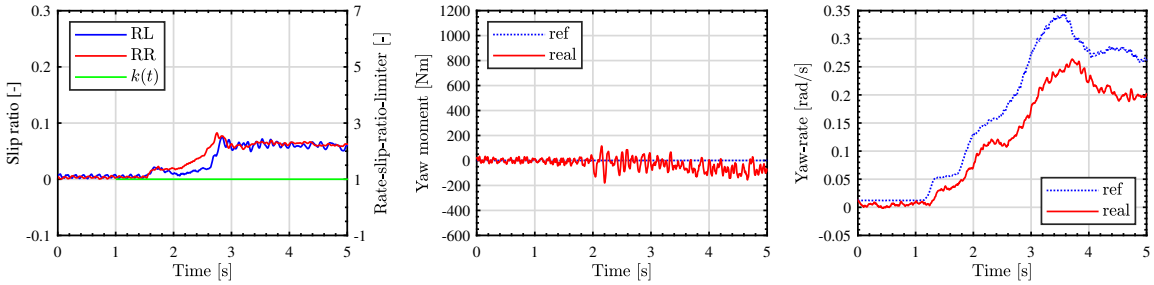

(a) Slip ratio and rate-slip-ratio-limiter. (b) Yaw moment. (c) Yaw-rate.

Fig. 8. Experimetal result of Case 1 (without yaw-rate control).

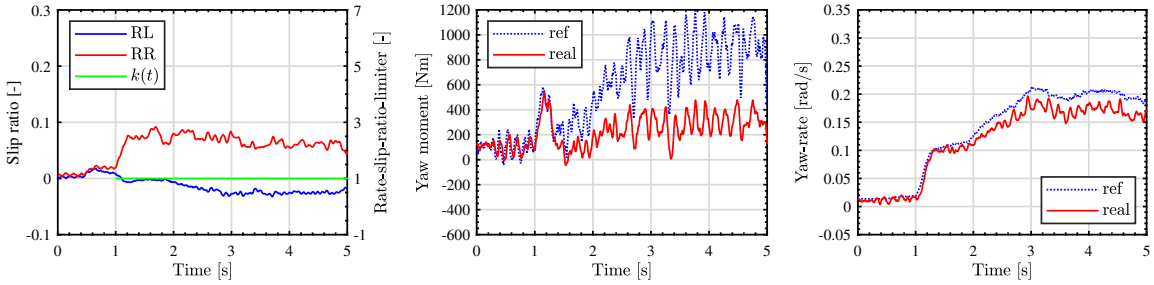

(a) Slip ratio and rate-slip-ratio-limiter. (b) Yaw moment. (c) Yaw-rate.

Fig. 9. Experimetal result of Case 2 (conventional DYC).

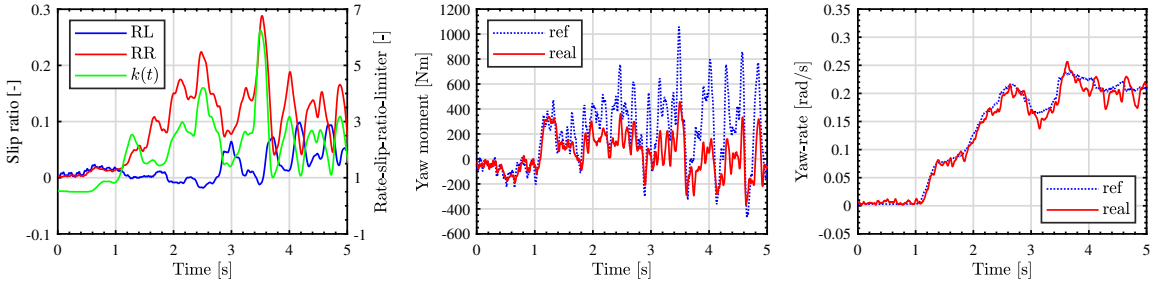

(a) Slip ratio and rate-slip-ratio-limiter. (b) Yaw moment. (c) Yaw-rate.

Fig. 10. Experimetal result of Case 3 (proposed DYC).